ELSEVIER

Optics and Lasers in Engineering 30 (1998) 527–537

OPTICS and LASERS in ENGINEERING

Whole-field digital measurement of principal stress directions in photoelasticity

T.Y. Chen*, C.H. Lin

Department of Mechanical Engineering, National Cheng Kung University, Tainan, Taiwan, Republic of China

Abstract

A method that uses three light-field isoclinic images and the associated light-field unloaded model (or white) images for whole-field digital determination of the principal stress directions in photoelasticity is presented. Relevant theory is derived and explicit conditions for directly determining the directions to the range 0–$\pi/2$ are given. Tests of this method on a directly loaded two-dimensional disc and a stress frozen photoelastic slice are demonstrated. The results agree well with the values obtained from the manual method and/or the theory.

Keywords: Photoelasticity; Principle stress directions; Whole-field digital measurement

1. Introduction

Photoelasticity is one of the most elegant methods for whole-field stress analysis. By using models made of birefringent materials, the difference and the directions of the principal stresses are given by isochromatic and isoclinic fringe patterns. Conventionally, principal stress directions are measured manually by rotating the polarizer and analyzer of a plane polariscope at the same time. In whole-field analysis, this measurement can be very tedious and require skill in the identification of isoclinic fringes.

Recent developments in the automated measurement of isoclinic parameters include using CCD (or TV) cameras, intensity measurement, polarization stepping, phase stepping, and digital image processing. Yao [1] used image division and image differentiation methods to extract the isoclinics. His method uses both plane and

*Corresponding author. Fax: 886-6-2352973; e-mail: ctyf@mail.ncku.edu.tw

0143-8166/98/$ - see front matter
PII: S0143-8166(98)00056-6

circular polariscope setups and many frames of isoclinics. Since quarter-wave plates are used, errors exist in this method due to dispersion in the quarter-wave plates. Brown and Sullivan [2] used four equally stepped isoclinic images (0, $\pi/8$, $2\pi/8$, $3\pi/8$) from a plane polariscope to measure the whole-field principal stress directions. In their study, the amplitude of light was found to vary with the polarizer angle, and the dark-field isoclinic images were normalized by using a separate set of four light-field plane polariscope images. The angles determined are in the range of ($\pi/8$, $-\pi/8$). Unwrapping of the results is required. Mawatari et al. [3] derived a single-valued representative function to determine the principal stress direction. They demonstrated the method using four polarization-stepped isoclinic images (0, $\pi/12$, $\pi/3$, $\pi/4$). The intensity distribution of the images were assumed to be independent of the polarizer angle. The determination of the principal stress angle from the function is relatively complicated. The feasibility of using four phase-stepped images from a circular polariscope to determine the isoclinic parameters of a stress frozen slice from a bolt was demonstrated by Patterson and Wang [4]. Sarma et al. [5] improved the phase stepping method by acquiring the isoclinic images at three analyzer positions in a plane polariscope with a monochromatic laser light source.

The polarization stepping method discussed above uses four frames of isoclinic images, and the measurements are made only on relatively simple two-dimensional shapes such as a disc under diametrical compression. In this paper, a method for whole-field automatic measurement of principal stress directions is proposed. To avoid the variation of light which occurs with different polarizer angles, the dispersion in the quarter-wave plates, and the high computer processing time, the method uses three light-field isoclinic images from a plane polariscope. Relevant photoelastic theory is derived. Tests of this method on a disc under diametrical compression and a frozen-stressed photoelastic slice are demonstrated. The results are in good agreement with results determined manually and theoretically.

2. Theory

In photoelastic experiments, the intensity of superimposed images of isochromatic and isoclinic fringes can be obtained from a plane polariscope. As shown in Fig. 1, the light-field intensity at an arbitrary point on a loaded model can be derived as [6]

$$I_{\mathrm{L}}(\theta) = I_{\mathrm{m}}(\theta)\,[1 - \sin^2 2(\phi - \theta)\sin^2(N\pi)], \tag{1}$$

where $I_{\mathrm{L}}(\theta)$ is the intensity of the light emerging from the analyzer, θ is the angle between the polarizer and an arbitrarily selected reference axis, $I_{\mathrm{m}}(\theta)$ is the maximum intensity of light emerging from the analyzer at angle θ, ϕ is the angle between a principal stress direction and the reference axis, $N\,(=\delta/\lambda)$ is the fringe order, δ is the relative retardation, and λ is the wavelength of the monochromatic light. For an unloaded model, the intensity can be represented as

$$I_{\mathrm{U}}(\theta) = I_{\mathrm{m}}(\theta). \tag{2}$$

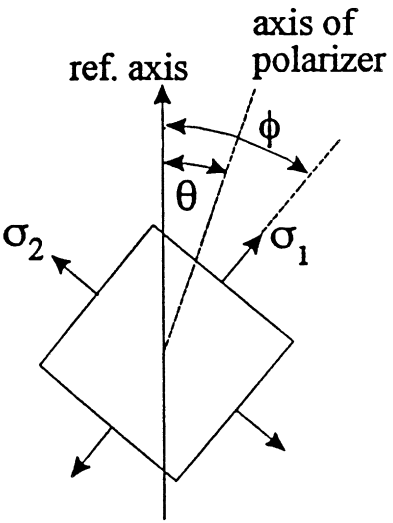

Fig. 1. Relationships between principal stress direction and relevant axes.

Then a dark-field normalized intensity of the loaded model I_1 can be calculated from Eqs. (1) and (2) as

$$I_1(\theta) = 1 - I_L(\theta)/I_U(\theta) = \sin^2 2(\phi - \theta)\sin^2(N\pi). \tag{3}$$

Similarly, if another two isoclinic images are acquired at angles $\theta + \pi/8$ and $\theta + \pi/4$, the dark-field normalized intensity of the two images can be obtained as

$$I_2(\theta + \pi/8) = \sin^2 2(\phi - \theta - \pi/8)\sin^2(N\pi). \tag{4}$$

$$I_3(\theta + \pi/4) = \sin^2 2(\phi - \theta - \pi/4)\sin^2(N\pi) = \cos^2 2(\phi - \theta)\sin^2(N\pi). \tag{5}$$

By adding Eq. (5) to Eq. (3), the following result is obtained:

$$I_1(\theta) + I_3(\theta + \pi/4) = \sin^2(N\pi). \tag{6}$$

It can be seen that the right hand side in Eq. (6) has the same form as the intensity representation of the isochromatic image in a circular polariscope. As pointed out by Mawatari et al. [3], $I_1(\theta)$ and $I_3(\theta + \pi/4)$ compensate each other, and Eq. (6) is useful to separate isochromatic fringes from isoclinic images obtained from the plane polariscope.

If $\sin^2(N\pi)$ in Eq. (3) is equal to zero (i.e., $I_1 + I_3 = 0$), no usable isoclinic information exists because the light intensity is virtually zero. Assuming that $\sin^2(N\pi) \neq 0$ (i.e., $I_1 + I_3 \neq 0$), then dividing Eq. (3) by Eq. (6), yields the value

$$I_1/(I_1 + I_3) = \sin^2 2(\phi - \theta) = [1 - \cos 4(\phi - \theta)]/2 \tag{7}$$

thus,

$$\cos 4(\phi - \theta) = (I_3 - I_1)/(I_1 + I_3). \tag{8}$$

By inverting Eq. (8), the principal stress direction can be obtained as

$$\phi = \theta + 0.25 \cos^{-1}[(I_3 - I_1)/(I_1 + I_3)]. \tag{9}$$

Since the range of ϕ determined from the above equation is $\pi/4$ ($\theta + \pi/8$ to $\theta - \pi/8$), phase unwrapping is required to bring the range to $\pi/2$. However, Eq. (4) can be rewritten as

$$\begin{aligned} I_2 &= \sin^2 2(\phi - \theta - \pi/8) \sin^2(N\pi) = [1 - \cos 4(\phi - \theta - \pi/8)] \sin^2(N\pi)/2 \\ &= [1 - \sin 4(\phi - \theta)] \sin^2(N\pi)/2 \end{aligned} \tag{10}$$

thus, dividing Eq. (10) by Eq. (6), yields

$$I_2/(I_1 + I_3) = [1 - \sin 4(\phi - \theta)]/2 \tag{11}$$

therefore,

$$\sin 4(\phi - \theta) = (I_1 + I_3 - 2I_2)/(I_1 + I_3). \tag{12}$$

Dividing Eq. (8) by Eq. (12), the principal stress direction can also be determined from the following equation:

$$\phi = \theta + 0.25 \tan^{-1}[(I_1 + I_3 - 2I_2)/(I_3 - I_1)]. \tag{13}$$

Again, the determined angle of ϕ here is in the range of $(\theta + \pi/8, \theta - \pi/8)$. By referring to the signs in Eqs. (8) and (12), and letting

$$V_s = \sin 4(\phi - \theta) \quad \text{and} \quad V_c = \cos 4(\phi - \theta),$$

the principal stress direction can be determined distinctly in the range 0–$\pi/2$ by the following six conditions:

$$\phi = \begin{cases} \theta + 0.25 \tan^{-1}(V_s/V_c) & \text{if } V_s \geqslant 0,\ V_c > 0, \\ \theta + 0.25 \tan^{-1}(V_s/V_c) + \pi/4 & \text{if } V_s \geqslant 0,\ V_c < 0, \\ \theta + 0.25 \tan^{-1}(V_s/V_c) + \pi/4 & \text{if } V_s \leqslant 0,\ V_c < 0, \\ \theta + 0.25 \tan^{-1}(V_s/V_c) + \pi/2 & \text{if } V_s \leqslant 0,\quad V_c > 0, \\ \theta + \pi/8 & \text{if } V_s > 0,\ V_c = 0, \\ \theta + 3\pi/8 & \text{if } V_s < 0,\ V_c = 0. \end{cases} \tag{14}$$

If the determined ϕ is greater than $\pi/2$, ϕ should be reduced by $\pi/2$.

3. System configuration and calibration

The system used is shown schematically in Fig. 2. It consists of a standard diffused-light plane polariscope for producing isoclinic images; a narrow-band filter with a center wavelength of 633 mm and a bandwidth of 10 nm for obtaining monochromatic images; a CCD camera (TM745, made by Pulnix America, Inc.) with

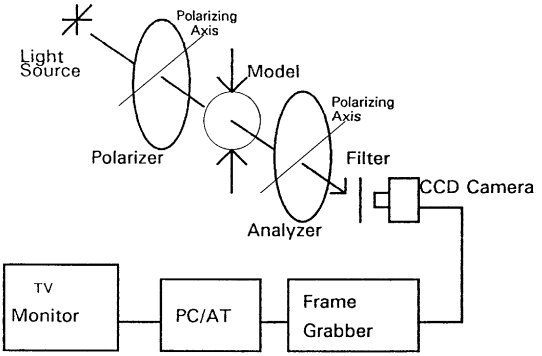

Fig. 2. Schematic of experimental setup.

a Micro-Nikkor 55 mm lens (made by Pokina Co., Japan); a frame grabber (Vision-Plus, made by Image Technology Inc.) with four frame buffers; a personal computer (IBM 486/DX2) with a 32-bit 66 Mz processor and 4 Mbytes of RAM, and other peripheral devices. Each frame buffer has 256 K bytes of memory that is organized as 512×512 pixels with 256 gray levels. The fringe pattern is presented to the CCD camera directly and is digitized at a rate of 30 frames/s. The system has been carefully calibrated by using a standard density-step tablet (made by Kodak Co.) [7]. The calibrated results were used to form a new look-up table for the acquisition of image data.

4. Experiments

In the two-dimensional experiment, the specimen used was a circular disk, 50 mm in diameter and 5 mm thick (made of photoelastic material, PSM-1). It was subjected to a concentrated diametrical load. The load was increased until four fringes appeared along the horizontal line across the center of the model in a light-field setting. With θ chosen to be zero, three isoclinic images and the three associated unloaded images were acquired for the angle of 0, $\pi/8$, and $\pi/4$ by rotating the polarizer and analyzer, respectively. Fig. 3a shows the three light-field isoclinic images of the loaded model observed through the paralleled plane polariscope setup. These images were obtained by averaging the intensity values of eight frames to reduce electronic noise. The area covered by each pixel is about 0.01 mm^2. Using Eq. (3), each light-field isoclinic image was processed into a normalized dark-field image. Since the values of the normalized dark-field image did not fall into the interval (0,1) exactly, the values were linearly adjusted before starting to calculate the principal stress directions. Firstly the minimum and maximum intensity values, $R_{\max}$ and $R_{\min}$, of the normalized image were found by comparing the intensity values of all points in the image. Then new values were calculated from the following equation:

$$S(x, y) = (R(x, y) - R_{\min})/(R_{\max} - R_{\min}), \tag{15}$$

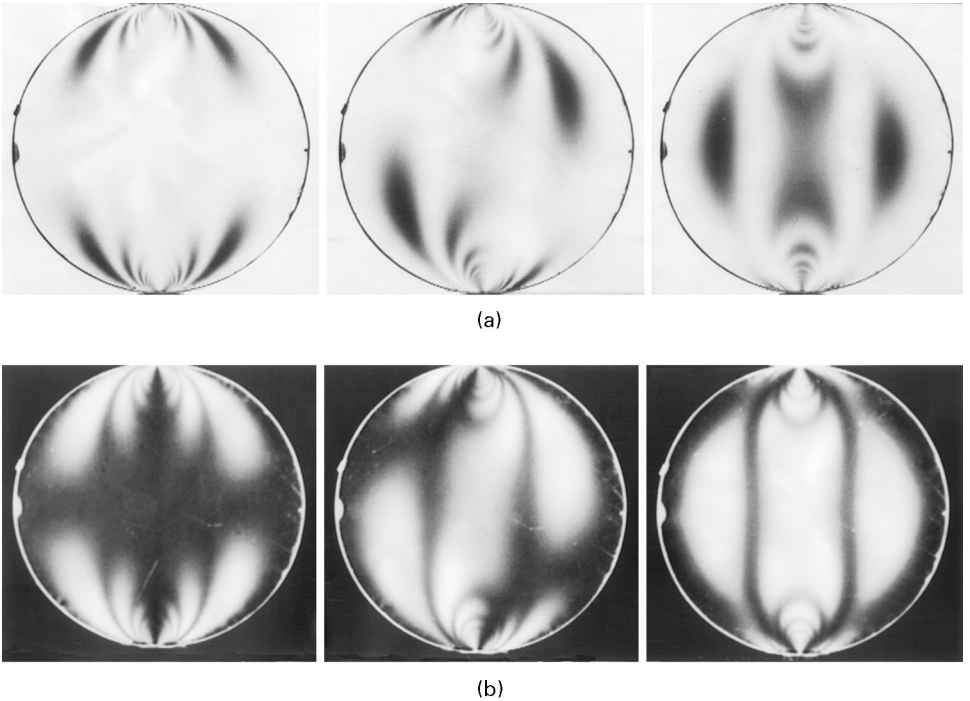

Fig. 3. (a) Light-field and (b) normalized and adjusted dark-field isoclinic images. From left to right: 0, $\pi/8$, $\pi/4$.

where $S(x, y)$ and $R(x, y)$ represent the new and old intensity values of a point located at (x, y). Thereafter the image values were used in Eqs. (8), (12), and (14) to determine the principal stress directions. Fig. 3b shows the normalized and adjusted dark-field images after being multiplied by 255.

In the frozen-stressed photoelastic slice experiment, a slice obtained from a full-scale model of a variable pitch lead screw at contact with two cylindrical meshing elements was used. The slice was a 1.2-mm-thick cut from the contact area for a contact stress study. Details of the preparation of the model and the stress-freezing procedures are described elsewhere [8]. The isoclinic images and the associated unloaded images were taken under the same angles as those used in the two-dimensional experiment. Fig. 4a shows a light-field isoclinic image of $\pi/8$. The resolution of the image is about 0.05 mm/pixel. Since the unloaded model image is not obtainable from a stress frozen slice, the normalization process has to be modified. Here the associated white image that was taken without the slice in the polariscope was used as the unloaded slice image. Fig. 4b shows the $\pi/8$ isoclinic image after being normalized, adjusted, and multiplied by 255. Thereafter the digital process for determination of the principal stress directions was the same as the procedures used in the two-dimensional case.

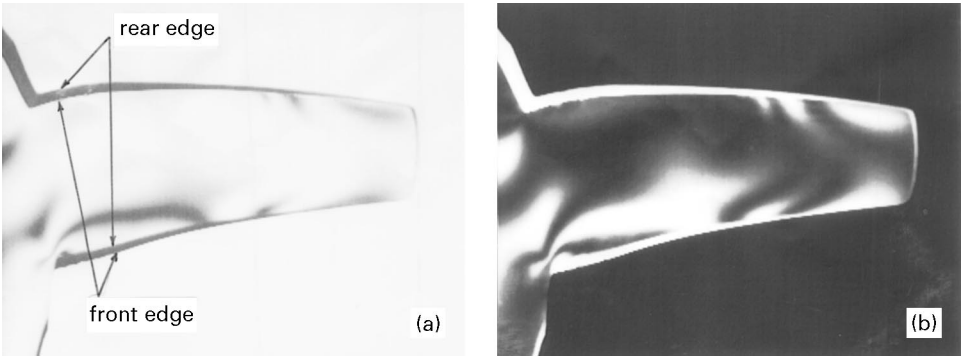

Fig. 4. (a) Light-field and (b) normalized and adjusted dark-field $\pi/8$ isoclinic images of a photoelastic slice.

5. Results and discussion

The purpose of using light-field isoclinic images in this study is to reduce the nonuniform distribution of light and the variation of the light that occurs with polarizer angle. It can be seen from Figs. 3b and 4b that the dark-field isoclinic images are good. The intensity values of isoclinic images were taken at angles of 0, $\pi/8$, and $\pi/4$, respectively. Generally any θ can be used to determine the principal stress direction ϕ, and the equations to be used are the same. For simplicity, θ was given the value of zero.

The outline of the slice used is shown in Fig. 4a. Since the thread surface curved sharply, the areas between the edges of the front and the rear surfaces reflect light. Thus, areas along the upper and lower edges appear dark in Fig. 4a and bright in Fig. 4b.

The determined principal stress directions of the circular disc, represented by nine gray levels, is shown in Fig. 5. It can be seen that the contour of isoclinics appear to zigzag at and near the isochromatic fringes. As mentioned previously, the reason for this is that there is no usable isoclinic information at and near the locations where the isochromatic fringes exist. In practice, the values at the zigzag were set to a neighboring value determined in an earlier step with the present designed algorithm. The zigzag effect looks larger as the isochromatic fringe becomes broader, and does not become stronger at the regions near the applied loads where the fringe density is higher. This effect can be reduced by filtering or curve fitting the data. If possible, one can apply smaller loads on the model to avoid producing isochromatic fringes and thus reduce the effect.

After being curve fitted by a polynomial using the regression method and interpolated or extrapolated numerically, the resulting principal stress directions were compared to those determined from the theory and the manual method. Fig. 6 shows the results along a horizontal line across the middle point of the upper-half disc. It can be seen that the agreement among them is quite good. The digitally determined values

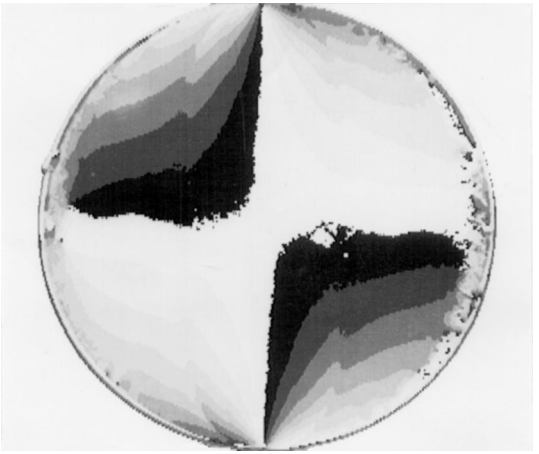

Fig. 5. Digitally determined principal stress directions of a disc, represented by nine gray levels.

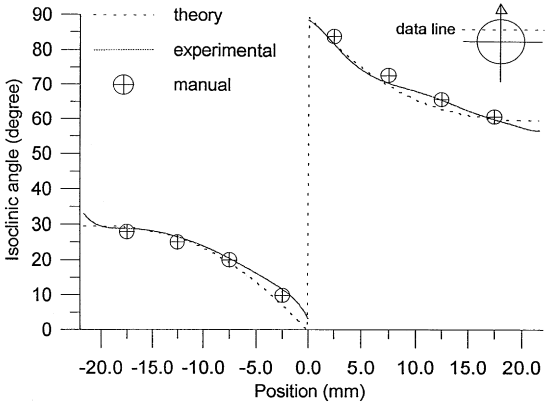

Fig. 6. Comparisons of the results from the experiment, theory, and the manual method.

of principal stress direction are closer to the values measured manually. The difference between the two is less than 2.8° except at regions near the isochromatic fringes.

Fig. 7 shows a gray-level representation of the digitally determined principal stress directions of the photoelastic slice. The gray-level values are obtained by multiplying the angle of degrees by 2. It can be seen that the gray level (principal stress direction) varies gradually in most areas. Errors are evident in the graph at or near the regions where the isochromatic fringes pass. Further comparison of the digitally determined principal stress directions along a horizontal line, indicated by an arrow in Fig. 7, with those determined from the manual method is shown in Fig. 8. It can be seen that the values obtained from both methods are in close agreement. As mentioned earlier, big

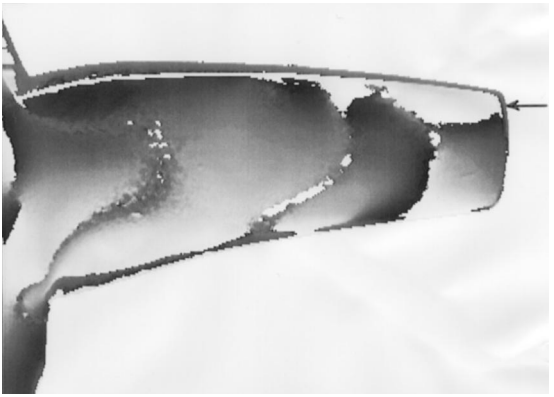

Fig. 7. Gray-level representation of the digitally determined principal stress directions of a photoelastic slice.

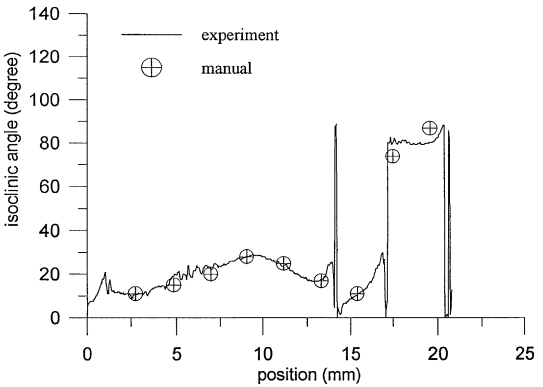

Fig. 8. Comparisons of the results from the experiment and the manual method.

errors occur at or near the fringe points, or near the edge. When only considering the nine data measured by both methods, the average difference is less than 3°, and the largest error is about 6°. Again, the points having larger errors can be reduced by digital filtering or curve fitting. However, it should be done with care because the angle of the principal stress direction jumps from 0 to 90°, and human intervention might be required.

In the slice measurement, the unloaded slice image was substituted by the white image in the normalization process. This modification is acceptable when the variation of light transmissibility in the slice is negligible. In the present study the normalized image values were found scaled down by the use of the modified process. However the scaling down effect was quite uniform except for some noise-like variations.

Generally the normalized image values did not fall into the interval (0,1) exactly. The reason for that is believed to be caused mainly by the effects of stray light, the digital process used in normalizing the photoelastic data, and the dark current generated in the CCD camera. In the linear adjustment process, the value of $(R_{max} - R_{min})$ in Eq. (15) was found varied for each image of I_1, I_2 and I_3 numerically. However the largest difference among them was found less than 5%. The influence of this difference on the determination of principal stress angle was examined by using Eq. (8). The results show that the errors caused on the determined principal stress angles are less than 1.5°. Therefore the adjustment process shifts the normalized values and would not incur appreciable errors.

Since only three frames of isoclinic image are required in our method and unwrapping is eliminated, the processing time should be less than that of the four-frame polarization-stepped method. It takes about 15 min to determine the whole-field (512×512) principal stress directions: 12 min are spent on the image normalization and computation to obtain dark-field isoclinic images; 3 min are used to compute the whole-field principal stress directions.

The computation system may be subject to various errors and thus affect the accuracy of the principal stress direction determined. Systematic and accidental errors that were added directly to the image data were readily eliminated through Eqs. (8) and (12), as long as the errors did not vary with θ. Since this was obviously not the case, the normalization process could be applied to the image data to reduce errors. It is also noted that the intensity at the low-light regions (less than 30) is not resolvable by this system, and errors might be generated. Use of a higher resolution camera would alleviate this problem. Another factor that may also affect the accuracy of measurements is quantization errors. The quantization error on the gray-level value is estimated to be less than 0.5, and is relatively small. Generally the data having relatively larger errors could be further improved by filtering or curve fitting.

6. Conclusions

A method for whole-field determination of the principal stress directions in photoelasticity is presented. Relevant theory is derived and six explicit conditions for directly determining the angle in the range $\pi/2$ are given. Tests of this method on a directly loaded two-dimensional disc and a stress frozen photoelastic slice demonstrate its usefulness. The results agree well with values obtained from the theory and the manual method. An accuracy of 2.8° is achievable through use of the proposed method.

Acknowledgement

The author is thankful to the National Science Council of the Republic of China for supporting this research under grants NSC84-2622-E006-005.

References

[1] Yao JY, Digital image processing and isoclinics. Exp. Mech 1990;30(3):264–9.
[2] Brown GM, Sullivan JL, The computer-aided holophotoelastic method. Expl Mech 1990; 30(2): 135–44.
[3] Mawatari S, Takashi M, Toyoda Y, Kunio T, A single-valued representative function for determination of principal stress direction in photoelastic analysis. Proc. 9th Intl Conf on Exp Mech. 1990;5:2069–78.
[4] Patterson EA, Wang ZF, Towards full field automated photoelastic analysis of complex components. Strain 1991;27(2):49–56.
[5] Sarma AV, Pillai SA, Subramanian G, Varadan TK, Computerized image processing for whole-field determination of isoclinics and isochromatics. Expl Mech 1992;32(1):24–9.
[6] Cloud G, Optical methods of engineering analysis. New York: Cambridge University Press, 1995.
[7] Chen TY. Digital fringe multiplication in three-dimensional photoelasticity. J Strain Anal 1995;30(1):1–7.
[8] Chen TY, Lin JS, Photoelastic stress analysis of a variable pitch lead screw, Proc. SEM Spring Conf. on Expl Mech. 1994:301–5.